

Uwe HEISEL¹
Thomas STEHLE¹
Hadi GHASSEMI^{1*}

EXPERIMENTAL INVESTIGATION INTO PARAMETERS INFLUENCING ROLL TENSIONING OF CIRCULAR SAW BLADES

Circular saw blades are rolled in the shape of a ring by special roll tensioning machines to improve the static and dynamic behaviour of steel saw blades. Plastic deformation and strain hardening in the roller track area cause residual stresses in the circular saw blade, which influence the static stiffness and the natural frequencies of the circular saw blade. Roll tensioning is one of the important parts when producing circular saws, especially in the production of thin circular saw blades. Although the influence of the roll tensioning process on the static and dynamic properties is well-known, it is interesting to further investigate the parameters influencing the roll tensioning process. This paper presents the influence of various parameters on the roll tensioning process, such as material properties, rolling force, contact condition between roller wheels and circular saw blade. These investigations help to find the optimisation ability of this process and to gain a better understanding of the relationships between roll tensioning processes and improved static and dynamic properties of thin saw blades.

1. INTRODUCTION

Circular saws are very widespread in wood machining. They are used in different batches and sizes from hand tools to large machining centres (CNC machines). The production process and the respective treatments in the production of saw blades are adjusted depending on the requirements on the cutting quality and the applications. Apart from tooth shape, tooth material and chip space of circular saws, axial vibrations of saw blades also have a significant impact on the quality of cutting edges and cut surface. The increasing demands on cutting quality, cutting performance and a better management of natural resources require thin, stable saw blade with minimum axial vibration amplitudes and high damping properties. These properties play a major role, particularly in the case of circular saw blades for wood machining because of the high operating speeds [1],[2]. Due to the high operating speed range, it is probable that the rotational frequency corresponds to a natural frequency and leads to resonance.

¹ University of Stuttgart, Institute for Machine Tools, Stuttgart, Germany.

* E-Mail: hadi.ghassemi@ifw.uni-stuttgart.de

Achieving a stable dynamic behaviour of the circular saw blade during cutting requires a high static stiffness and damping ratio for steel blades. To meet this goal, it is not only necessary to correctly select the saw blade material but also to carry out heat treatments for increasing the hardness and elasticity properties of saw blade. However, the material properties have only limited influence on circular saw blades due to their shape, i.e. their thickness is very small compared with the diameter. Furthermore, the thermal and centrifugal stresses which occur during the cutting process negatively influence the dynamic behaviour of the saw blade. The pretensioning of circular saw blades by roll tensioning and thus the induction of residual stresses into the material is an empirically and scientifically accepted method to improve the static and dynamic properties of circular saw blade. Roll tensioning can reduce the circular saw blades' thickness up to 40% as compared to those which have not undergone roll tensioning [3]. The oldest known method for generating residual stresses in circular saw blade is based on the generation of stresses in the central zone by hammering [4]. However, this method is very inaccurate since neither the force applied by hammering nor the exact exposure time of the force is determined. For this reason, in 1955 the Institute for Tool Research in Remscheid has already begun to develop a uniform procedure for inducing residual stresses into saw blades. Machine tensioning of circular saw blades has made it possible to induce a uniform residual stress distribution and a reproducible process operation [5]. This method is still prevalent.

As illustrated in Fig. 1, the roll tensioning machine principally consists of two rollers, which are located exactly on top of each other, and a specific sliding carriage with a centre, that can be axially adjusted by a stepper motor and rotate due to roller bearings. This makes the circular saw blade to rotate freely on the sliding carriage during the rolling process, and the roll radius can be adjusted at will by the stepper motor.

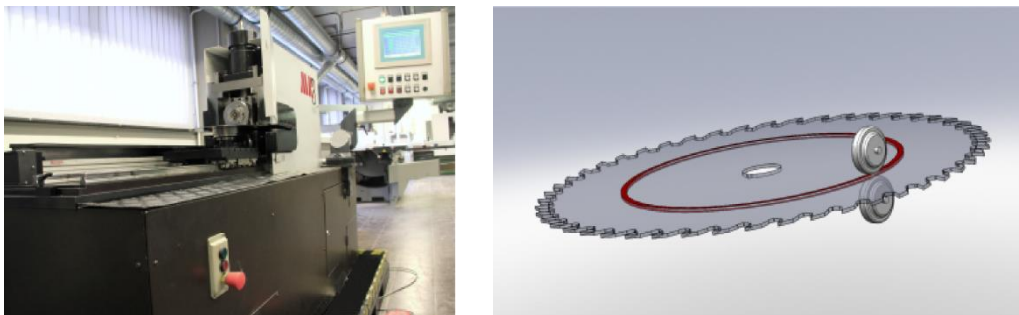


Fig. 1. Roll tensioning machine (left) and schematic representation of roll tensioning (right)

The upper roller is vertically adjustable and rotatable, but the lower roller is only rotatable. The rolling force is applied by means of hydraulic pressure through the upper roller. Roll tensioning begins as soon as the defined rolling force is achieved. Then both of the rollers begin to rotate in the opposite direction, making the circular saw blade turn due to stiction.

For a better understanding and optimization of the roll tensioning process, fundamental studies about the parameters influencing this process were carried out. This paper presents

the investigations into the material properties of saw blades, the tribological contact conditions between contact pairs and the influence of variation on rolling force. The investigated sample materials here correspond to the conventional saw blade material used in the production of circular saws. Material and dimension specifications of the circular plates are shown in Table 1. Table 2. Gives the composition of the sample material according to the manufacturer's data.

Table 1. Material and dimension specifications of the tested circular plates

Material	75 Cr1 (1.2003)
External diameter	300mm
Inside diameter	30mm
Thickness	1.6mm

Table 2. Material composition of the investigated circular saw blade (75Cr1)

C	Si	Mn	P	S	Cr	Mo	Ni	V	W
0.74- 0.80	0.25- 0.40	0.65- 0.80	< 0.025	< 0.010	0.30- 0.45	-	-	-	-

2. EXPERIMENTAL DETERMINATION OF MATERIAL PROPERTIES

In order to achieve specific material properties, the circular saw blade must be rolled, hardened and ground during the production process. Hence, a 100 percent homogeneity of the material can be ruled out due to this process. An accurate statement of the isotropic or anisotropic properties can be made by determining the material properties. The universal tensile test machine (see Fig. 2) is used to carry out the tensile tests for determining the material properties. The test procedure is automated by the test software, according to DIN EN ISO 6892-1. First, the test specimen is slowly loaded with a preload of 10MPa. Subsequently, the load is continuously increased until the sample breaks. At 80MPa preload force, the increased ratio of the force as per time is 20MPa/s and increases to 30MPa/s in the elastic region. Finally, the increase reaches 48MPa/s, the breaking point.

The sample forms are also manufactured according to DIN 50125. The samples were cut out from a rectangular plate in three different directions through water jet cutting process in order to verify the material anisotropy, so that no thermal stress could affect the results of the tensile tests. The samples were cut at an angle of 0° in the grinding direction of the rectangular plate (longitudinally), at an angle of 90° to the grinding direction (transversely) and at an angle of 45° (diagonally). Then the samples were ground in accordance with DIN 50125 for achieving the required roughness. Fig. 2 also shows a sketch of the prepared samples. A total of 18 samples were tested (i.e. 6 samples in each direction). Arithmetic means, standard deviations and relative deviations from the measured values were analysed to evaluate the directional dependence of material properties and the measurement accuracy. The evaluation was carried out among the cut samples in the same directions and then among samples in all directions. The variations in the measurement

conditions and in the material structure of each sample lead to random errors. By arithmetic mean (equation 1), the random errors are partially compensated [6].

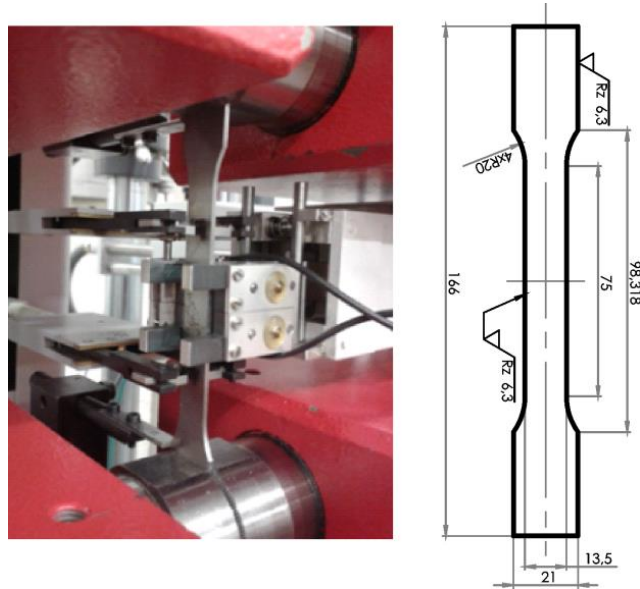


Fig. 2. Universal tensile test machine and sketch of the tensile test sample

$$\bar{a} = \frac{1}{n} \sum_{i=1}^n a_i \tag{1}$$

The arithmetic means of the tensile test results are listed in Table 3.

Table 3. Arithmetic means of material properties in all directions

Direction of the samples	Young's modulus E [MPa]	Yield stress $R_{p0,2}$ [MPa]	Ultimate stress R_m [MPa]	Poisson's ratio ν
Longitudinal (0° Sample)	204.016	1,263.36	1,435.09	0.283
Diagonal (45° Sample)	209.716	1,233.74	1,429.80	0.329
Transverse (90° Sample)	214.932	1,247.45	1,440.46	0.229

A measure for evaluating the scattering of the measured values is the standard deviation defined by Gauss. The standard deviation can be defined for individual values and arithmetic mean values. The individual value standard deviation (equation 2) is a measure of how the respective measurement values are scattered around its mean [7]. Arithmetic mean value standard deviation (equation 3) is a measure of the uncertainty of the mean from the true value [8].

$$\delta_a = \sqrt{\frac{1}{n-1} \sum_{i=1}^n (a_i - \bar{a})^2} \quad (2)$$

$$\delta_{\bar{a}} = \frac{1}{\sqrt{n}} \delta_a \quad (3)$$

This means here that the standard deviation from the individual value assesses the deviation among measured values of 6 samples and its average per direction. Equation 3 makes it clear that the standard deviation from the mean decreases as the number of measured values or tests increases. The relative standard deviation from the mean is calculated as follows:

$$\Delta_{\delta_a} = \frac{\delta_{\bar{a}}}{\bar{a}} \cdot 100 \% \quad (4)$$

Table 4 gives the calculated value of standard deviations and relative standard deviation of the material properties for the investigated samples in all three directions.

Table 4. Calculated standard deviations and relative standard deviation of the measured values per direction

Direction of the samples	Deviation of E-Modulus			Deviation of yield stress			Deviation of ultimate stress		
	δ_E [MPa]	$\delta_{\bar{E}}$ [MPa]	Δ_{δ_E} [%]	$\delta_{R_{p0,2}}$ [MPa]	$\delta_{\bar{R}_{p0,2}}$ [MPa]	$\Delta_{\delta_{R_{p0,2}}}$ [%]	δ_{R_m} [MPa]	$\delta_{\bar{R}_m}$ [MPa]	$\Delta_{\delta_{R_m}}$ [%]
Longitudinal (0° Sample)	3.424	1.398	0.69	11.93	4.87	0.39	7.34	3.00	0.21
Diagonal (45° Sample)	1.726	704	0.34	3.95	1.61	0.13	2.05	0.84	0.06
Transverse (90° Sample)	3.436	1402	0.65	3.44	1.40	0.11	2.90	1.18	0.08

The results generally show a very small scattering of measurements (below 1%). Particularly the samples in diagonal direction show the smallest scattering. To assess the isotropy or anisotropy of the material properties, the absolute and relative deviations between the conventional Young's modulus of steel ($E_{\text{steel}} = 210.000 \text{ MPa}$) and the measured mean values of Young's modulus per sample direction have been calculated using equations 5 and 6. These values are listed in Table 5.

$$(F_{abs.})_E = \bar{E} - E_{\text{Stahl}} \quad (5)$$

$$(F_{rel.})_E = \frac{\bar{E} - E_{\text{Stahl}}}{E_{\text{Stahl}}} \cdot 100 \% \quad (6)$$

Table 5. Relative and absolute deviation between the Young's modulus of the measured mean values per direction and conventional value of Young's Modulus of steel

Direction of the samples	Relative deviation	Absolute deviation
	$(F_{rel.})_E$ [%]	$(F_{abs.})_E$ [MPa]
Longitudinal (0° sample)	-2.85	-5.984
Diagonal (45° sample)	-0.13	-284
Transverse (90° sample)	2.35	4.932

The very small relative deviations rule out anisotropic material properties in the studied samples.

3. TRIBOLOGY PROPERTIES BETWEEN ROLLER WHEEL AND SAW BLADE

The assumption, which only pure rolling occurs between the contact pairs, is theoretically justified. In reality, contact between contact pairs is always superimposed by sliding. In general, the superimposed sliding friction between contact pairs can be macroscopic or microscopic [9]. Hence, due to this sliding effect a part of the rolling force is converted into heat instead of forming the saw blade.

The roller wheel includes two radii of curvature. These are the 'rolling radius', which is perpendicular to the axis of rotation, and the 'crowning radius', which describes the curvature of the surface on the roller wheel. The crowned surface of roller wheel causes different perpendicular distances between roller wheel surface and axis of rotation so that it reaches its maximum value at the top of the roll crown (middle of the contact area) and decreases in the direction of the roller wheel edge. This results in different peripheral speeds on the roller wheel surface and the corresponding slip on the contact surface. In this way, the rolling contact of the contact area is superimposed by sliding, which increases in the direction of the roller wheel edge.

The friction factor can be measured by using a strip-pulling system (see Fig. 3). A hydraulic cylinder presses the tool on top of the strip sample. The strip samples are clamped on a sledge and drawn underneath the tool by a linear actuator.

The friction force and the normal force can be measured by means of strain gauges and the piezoelectric sensors. Consequently, the surface pressure, defined as the ratio of the normal force F_N and drawing jaw surface S_B (equation 7), can be calculated:

$$\sigma_A = \frac{F_N}{S_B} \quad (7)$$

The investigated strip samples are made of saw blade material (see Table 1.) and the drawing jaw is made of roller wheel material (material number 1.2379). The friction coefficient μ is calculated according to Coulomb's law from the ratio between friction force F_R and normal force F_N (Equation 8).

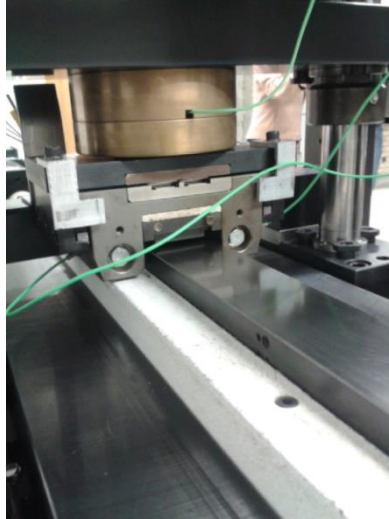


Fig. 3. Strip-pulling machine

$$\mu = \frac{F_R}{F_N} \quad (8)$$

To determine the friction coefficient, the examinations were carried out for both the dry state and the lubricated condition with one to three drops of lubricant, where 40 drops correspond to 1 gram of the lubricant used. Platinol B804/3 COW-1 was used as a lubricant here. The study of the friction coefficient in lubricated condition is interesting to the extent that there can still be some lubricant on the circular saw blade during the production process, depending on the pre-treatment. This has a great influence on the sliding friction coefficient, as will be shown below. The experiment in dry state was carried out with drawing jaws surfaces of 1.200 and 150mm². In this way, the influence of the contact areas and the surface pressure on the friction coefficient could be studied.

The tests in the dry state must be very carefully performed with gradual increase of normal forces to prevent adhesion occurring or to recognize it in time. A decrease in the sliding friction coefficient from dry to lubricated state by about 66% is clearly visible. The determined arithmetic means of the sliding friction coefficient μ_G in dry and lubricated state are shown in Table 6.

Table 6. Arithmetic means of the measured sliding friction coefficient

Dry state			Lubricated state			
Normal force F_N [KN]	Jaw surface S_B [mm ²]	Sliding friction coefficient μ_G	Drop number	Normal force F_N [KN]	Jaw surface S_B [mm ²]	Sliding friction coefficient μ_G
6	1.200	0.146	3	30	150	0.040
30	1.200	0.138	2	30	150	0.051
15	150	0.157	1	30	150	0.053
30	150	0.130				

The maximum relative deviation from the mean of all measured values in the dry state is less than 10% and in the lubricated state is 16.7%, although the sliding friction coefficient decreased with the number of drops of lubricant. The comparison between the sliding friction coefficients at different jaw areas at the same normal force shows a rising sliding friction coefficient with increasing jaw areas. The arithmetic mean of the measured value of sliding friction coefficients at a dry state is 0.143 and 0.048 in the lubricated state. The arithmetic means of the static friction coefficient are determined in the dry state at 0.151 and 0.051 in the lubricated state. As shown in Fig. 4, the friction force stays approximately constant. This fact is valid for both cases (dry and lubricated state) and regardless of the normal force.

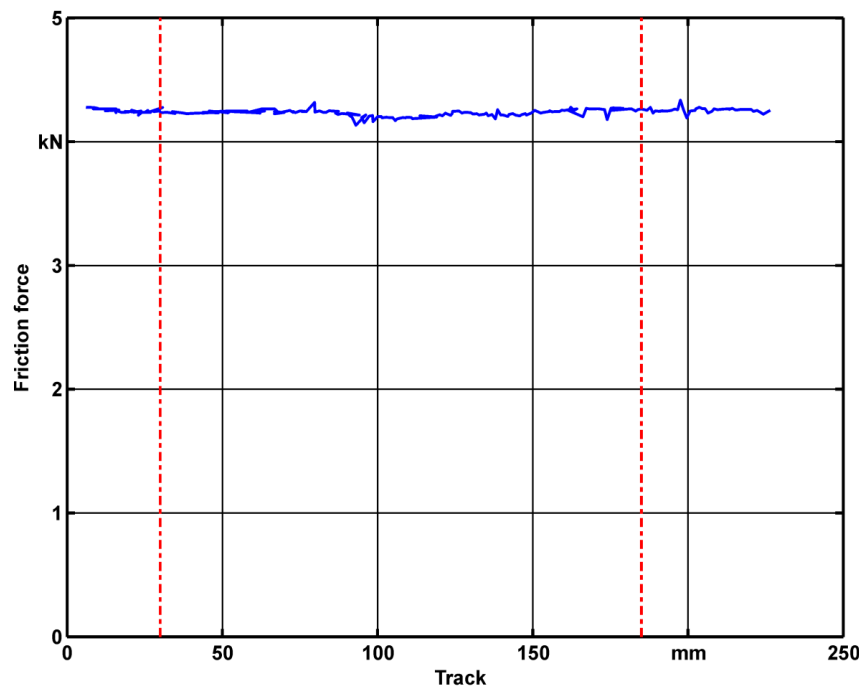


Fig. 4. Friction force in the dry state at 200MPa surface pressures

4. INFLUENCE OF THE ROLLING FORCE

The amount of the induced residual stress in the circular saw blade is mainly influenced by the rolling force. A very low rolling force causes poor pretensioning of the circular saw blade, and large rolling forces bend the circular saw blade and profoundly affect the run-out. Both cases can lead to great axial vibrations and hence to instability, quality deterioration and even safety problems, particularly in the case of circular saw blades in wood machining which are operated at very high rotational speeds. Hence, the following experimental investigations demonstrate the influences of the rolling force on the decreasing thickness in rolling track and the induced residual stress due to roll tensioning.

The decrease in thickness in the rolling track zone can cause stress concentrations in the necking area (notch effect). The decrease in thickness because of the different rolling forces is determined using a visual 3-D measuring system. The operating principle of this 3-D measuring system is based on the detection of the surface structure of the specimen and the assignment of the coordinates of the respective pixels. For this so-called raster scan method, the application of a stochastic spray pattern on the sample surface is required. The equipment software recognizes the shifts in the spray pattern and can compare the recordings of the initial state with the recordings after the roll tensioning and consequently calculate the resulting strains. The cameras of the instrument can be freely positioned above the test specimen by a tripod and measures the strains in all three directions [10],[11]. The measured strains in all three directions can be represented as a coloured image and measurement data. Furthermore, the number of measurement points can be set. Fig. 5 shows a strain pattern in cross-direction to the direction of rolling as a result of the rolling force of 7.848N.

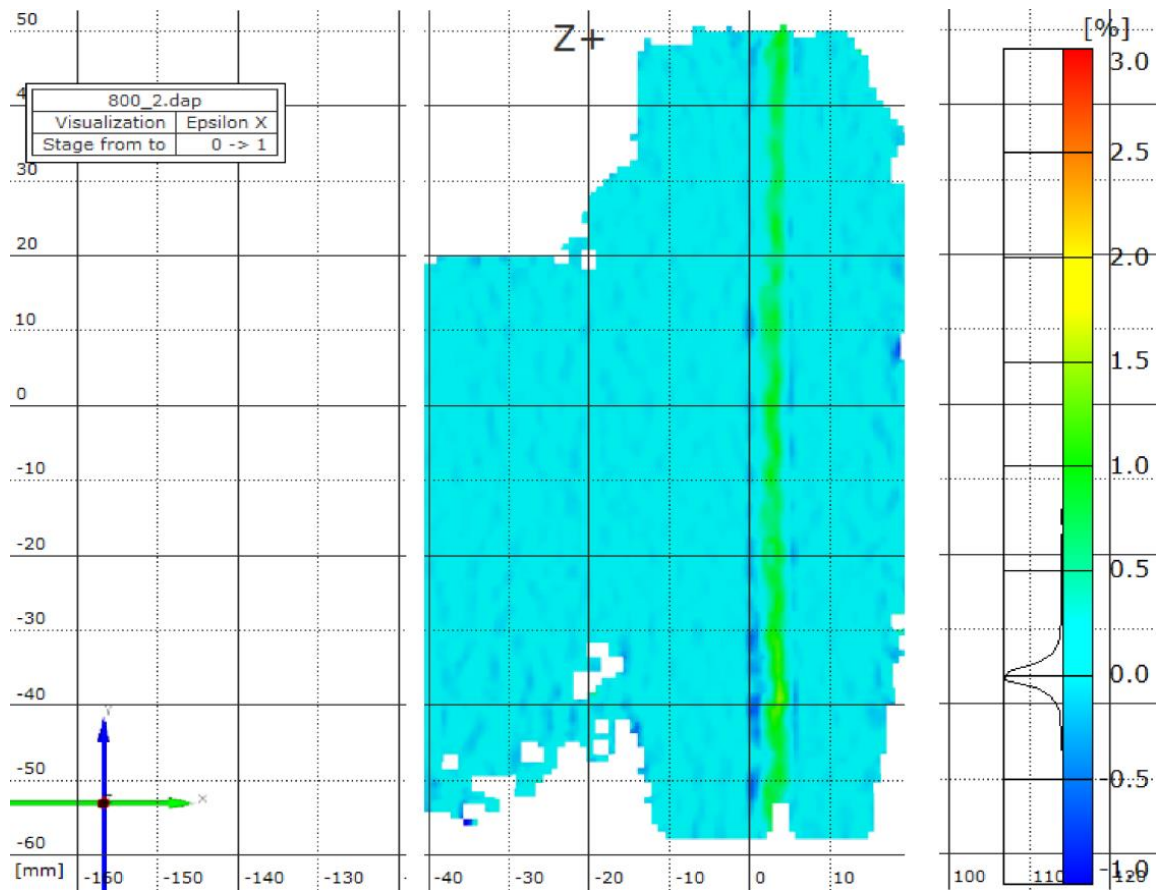


Fig. 5. Strain in the x-direction due to a rolling force of 7.848N

For these investigations, rectangular plates of 75 Cr1 (see Table 2.) with plate thickness of 1.6mm were used and rolled at different forces. A bend of the plate was

detected from a rolling force of 9.810N. This force defines the upper limit for the rolling force. The measured rolling depths along the plate width are illustrated in Fig. 6.

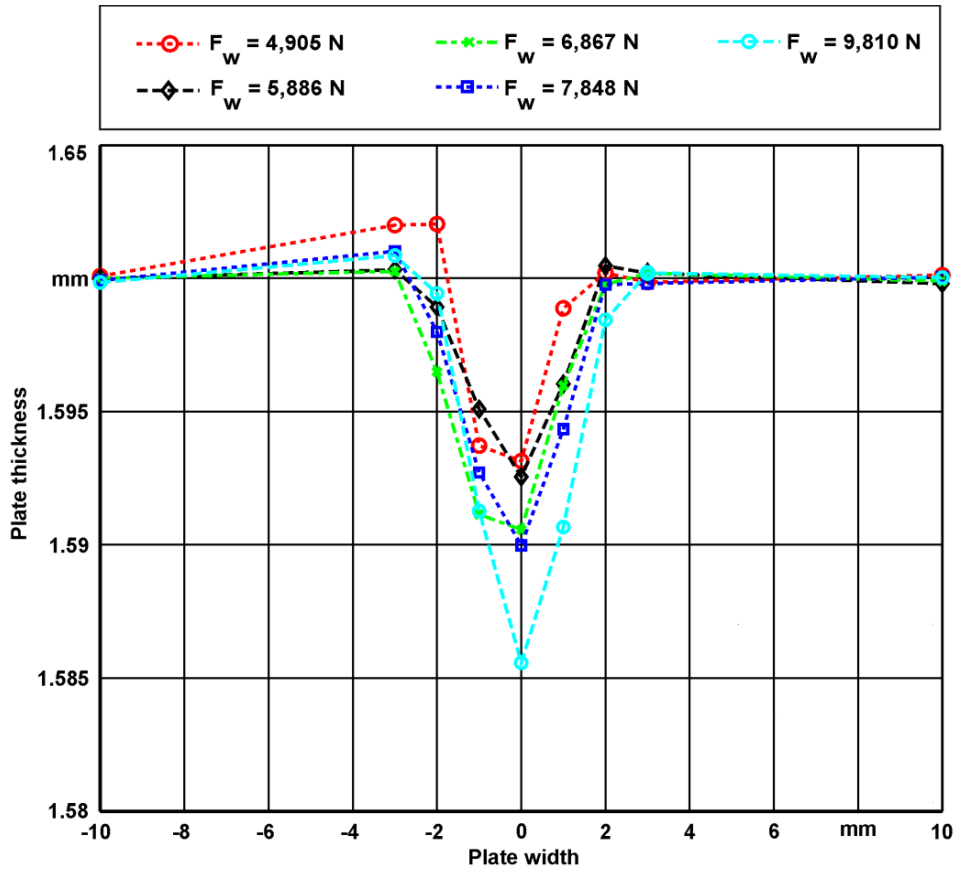


Fig. 6. Decreasing thickness of the plate in the rolling track due to rolling force variations

Both the rolling track depth and the rolling track widening can be gathered from Fig. 6. By subtracting the thickness (after rolling) from the initial thickness (1.6mm), the respective decrease in thickness is determined (see Table 7).

Table 7. Rolling track depth depending on rolling force variation

Rolling force F_w [N]	Rolling track depth [mm]
4.905	0.0069
5.886	0.0075
6.867	0.0094
7.848	0.0100
9.810	0.0144

As expected, the rolling track depth increases with increasing rolling force. But due to non-linear material properties in the plastic region, this increase is non-linear (see Fig. 7).

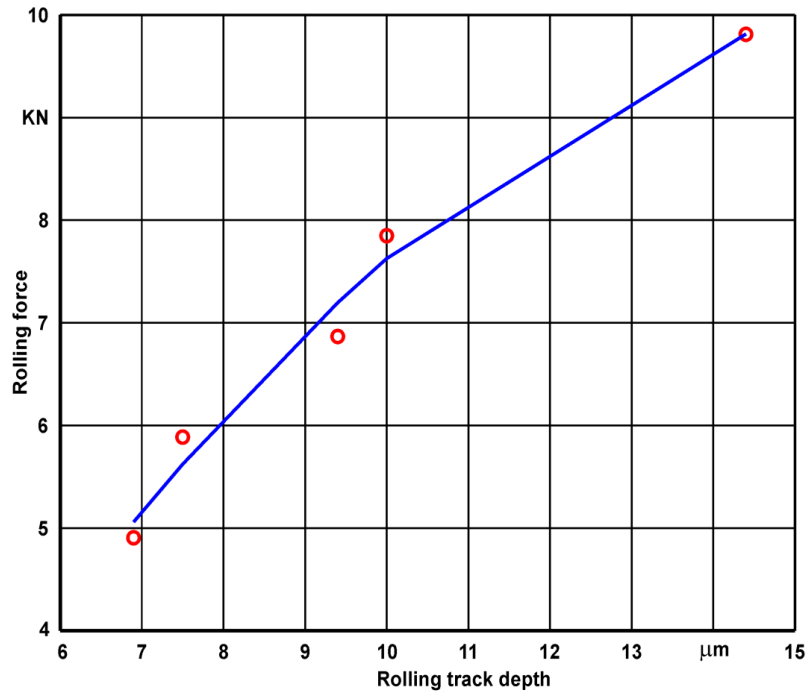


Fig. 7. The rolling track depth depending on the rolling force

The residual stress gradients due to the rolling force variation are determined by means of strain gauges. The effect of strain gauge is based on the change of the electrical resistance due to the occurring strain by tensile or compressive stresses [12]. For these investigations, circular plate of 75Cr1 (see Table 1) were used. The measurements were made with eight pieces of strain gauges rosettes, applied at different radii of the circular plate (see Fig. 8). The strain gauges were applied as close to each other as possible, so that curve progression of residual stress could be determined very well. According to Fig. 8, the circular plate can be divided into three zones, i.e. inner ring, rolling track zone and outer ring.

The strain gauge rosette consists of two strain gauges that are at 90 degrees to each other, and measure the strains in the radial and tangential direction. To calculate the radial and tangential residual stresses from measured strains by strain gauges, equation 9 was used [13].

$$\begin{cases} \sigma_r = \frac{E}{1-\nu^2} (\varepsilon_r + \nu \cdot \varepsilon_t) \\ \sigma_t = \frac{E}{1-\nu^2} (\varepsilon_t + \nu \cdot \varepsilon_r) \end{cases} \quad (9)$$

Here it needs to be mentioned, that the two conditions required to arrive at equation 9 are isotropic material properties and elastic strain. Both these conditions have been maintained here except of rolling track zone. In the rolling track, the circular plate is

plastically deformed and furthermore any contact between roller wheel and the strain gauge destroys strain gauge. Therefore it is not possible to measure the strains in the rolling track by using this method.

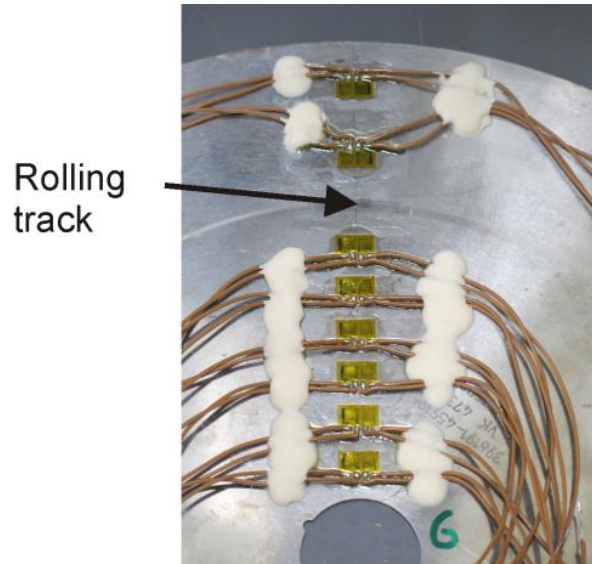


Fig. 8. Arrangement of strain gauges on the circular plate

The circular plates were rolled at a radius of 100mm ($2/3$ of the external radius of the circular plate) with 4.905 and 7.848N. After measuring the radial and tangential strains, the corresponding residual stresses were calculated according to equation 9 for the measured radii and the residual stress progression was displayed using the method of the least square error with the help of MATLAB.

The centrifugal and thermal stresses during the cutting process cause radial tensile stresses in circular saw blades. The tangential stress is tensile stress in the case of centrifugal force. Due to thermal stresses, strong tangential compressive stresses are produced in the edge region [14]. But as shown in Fig. 9, the curve trace of induced residual stresses due to pretensioning of the circular saw blade by roll tensioning are exactly reverse to the centrifugal and thermal stresses (above-mentioned) occurring during the cutting process. This fact leads to partially stress compensation in the circular saw blade during cutting process. Therefore, a possible precise adjustment of the rolling force, to optimal pretension of the circular saw blade, is desired.

According to Fig. 9, due to roll tensioning process a tangential tensile is induced in the outer ring and a radial compressive stress in both the rings as residual stress. These curves are shown here depending on relative radius r_b , which is defined as the radius r in relating to the circular plate radius of $r_a = 150\text{mm}$ (see equation 10).

$$r_b = \frac{r}{r_a} \quad (10)$$

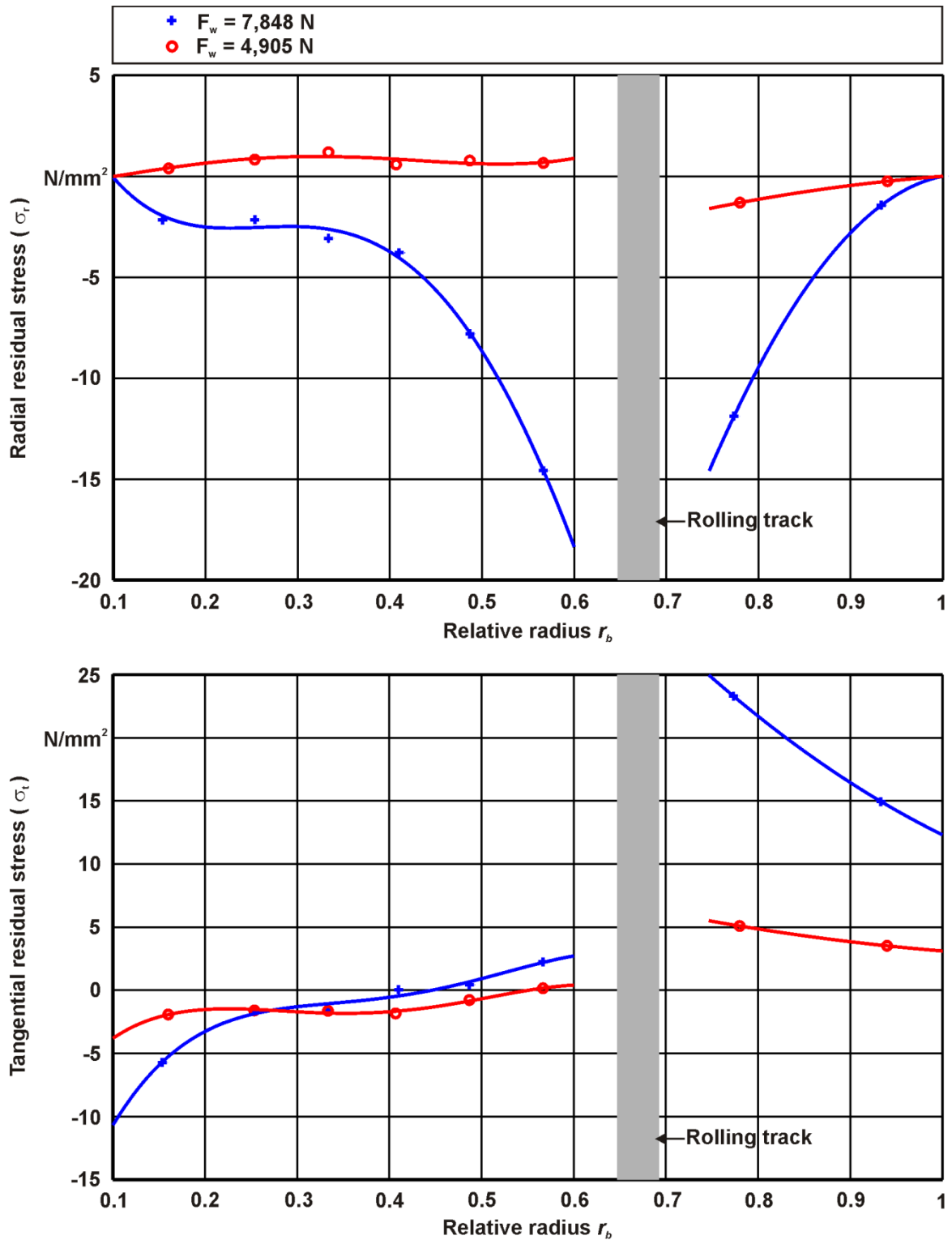


Fig. 9. Radial and tangential residual stresses in the circular plate depending on rolling force variation

While a rolling force of 4.905N cannot induce sufficient residual stresses, an approximate of 3KN greater rolling force improves the radial and tangential residual stress progression considerably (see Fig. 9).

5. SUMMARY

The investigations carried out here serve as a basis for better understanding of the roll tensioning and its influence on the improvement of dynamic behaviour of circular saw blades. First of all, the material properties of conventional circular saw blades for wood working and tribological influence between roller wheels and circular saw blade were investigated experimentally. The results could prove an isotropic material behaviour of the investigated circular saw blade material. The theoretical assumption of pure rolling friction between roller wheel and circular saw blade is very idealistic. In reality, the pure rolling friction is always overlaid with a sliding friction. In addition, the respective friction coefficients were found out under consideration of the different contact condition scenarios here. These results are used in the construction of the simulation model of roll tensioning process.

Based on the experimental stress analysis of the circular saw blade is possible to find the optimal rolling force at the roll tensioning, which induces tailor-made residual stresses in the circular saw blade. The results show that it is possible to compensate, by means of suitable roll tensioning parameters, the stresses caused during cutting process by centrifugal and thermal load in circular saw blade. Finally, these findings can lead to improve the cut quality and a safe operation of the circular saw blades.

For further investigation, a comparison between experimental and simulative determined residual stresses are planned. Furthermore, the relationships between the induced residual stresses and displacement of the natural frequencies of the circular saw blade will be studied.

REFERENCES

- [1] HEISEL U., STEHLE T., BIRENBAUM C., 2011, *Simulation und experimentelle Untersuchung von Kreissägeblättern*, In: Holztechnologie, 52, 15–21.
- [2] HEISEL U., STEHLE T., BIRENBAUM C., GHASSEMI H., 2013, *Simulative Untersuchung von Kreissägeblättern*, In: wt Werkstattstechnik online, 103, 69–75.
- [3] SCHAJER G.S., MOTE Jr. C.D., 1983, *Analysis of roll tensioning and its influence on circular saw stability*, Wood Sci. Technol., 17, 287–302.
- [4] ETTTEL B., GITTEL H.J., 2004, *Sägen, Fräsen, Hobeln, Bohren: Die Spannung von Holz und ihre Werkzeuge*, DRW-Verlag.
- [5] BARZ E., 1963, *Vergleichende Untersuchungen über das Spannen von Kreissägeblättern mit Maschinen und mit Richthämmern*, Holz als Roh- und Werkstoff, 21, 135–144.
- [6] EICHLER H.J., KRONFELDT H.D., SAHM J., 2004, *Das neue physikalische Grundpraktikum*, Springer Verlag
- [7] BANTEL M., *Messgerätepraxis*, Fachbuchverlag Leipzig.
- [8] PITKA R., BOHRMANN S., STÖCKER H., TERLECKI G., ZETSCHKE H., 2009, *Physik Der Grundkurs*, Verlag Harri Deutsch.
- [9] BIRKHOFFER H., KÜMMERLE T., 2011, *Feststoffgeschmierte Wälzlager - Einsatz, Grundlagen und Auslegung*, Springer Verlag.
- [10] ARAMIS Benutzerhandbuch Software, 2007, Braunschweig: GOM mbH.
- [11] ARAMIS Benutzerinformation Hardware, 2008, Braunschweig: GOM mbH.
- [12] LEÓN F. P., KIENCKE U., 2012, *Messtechnik, Systemtheorie für Ingenieure und Informatiker*, Springer Verlag.
- [13] KESSEL S., FRÖHLING D., 2012, *Technische Mechanik-Engineering Mechanics*, Springer Verlag.
- [14] PAHLITZSCH G., FRIEBE E., 1973, *Über das Vorspannen von Kreissägeblättern*, Holz als Roh- und Werkstoff, 31, Springer Verlag, 429–436.